Plant Physiol. (1996) 112: 1089–1100

Pressure Regulation of the Electrical Properties of Growing *Arabidopsis thaliana* L. Root Hairs[1]

Roger R. Lew*

Department of Biology, York University, 4700 Keele Street, North York, Ontario, Canada M3J 1P3

Actively growing *Arabidopsis thaliana* L. (Columbia wild type) root hairs were used to examine the interplay between cell turgor pressure and electrical properties of the cell: membrane potential, conductance, cell-to-cell coupling, and input resistance. Pressure was directly modulated using a pressure probe or indirectly by changing the extracellular osmolarity. Direct modulation of pressure in the range of 0 to about 15×10^5 Pa (normal turgor pressure was $6.8 \pm 2.0 \times 10^5$ Pa, $n = 29$) did not affect the membrane potential, conductance, coupling, or input resistance. Indirect modulation of turgor pressure by adding (hyperosmotic) or removing (hypo-osmotic) 200 mM mannitol/sorbitol affected the potential and conductance but not cell-to-cell coupling. Hypo-osmotic treatment depolarized the potential about 40 mV from an initial potential of about −190 mV and increased membrane conductance, consistent with an increase in anion efflux from the cell. Hyperosmotic treatment hyperpolarized the cell about 25 mV from the same initial potential and decreased conductance, consistent with a decline in cation influx. The results are likely due to the presence of an "osmo-sensor," rather than a "turgor-sensor," regulating the cell's response to osmotic stress.

Water relations are a key determinant of growth and development in plants (Milthorpe and Moorby, 1974; Kramer, 1983). Water movement through higher plant cells is one of the steps in its transport throughout the plant (Passioura, 1988), and net water movement into the cells, partly due to ion accumulation inside the cell, creates an internal hydrostatic pressure (turgor) that is a driving force for cell growth by expansion (Cosgrove, 1986). Whether or not cellular expansion is occurring, plant cells normally maintain a high internal hydrostatic pressure, which can be modified by ion transport and water movement through the plant. It is clear that regulation of water relations at the level of the single cell is closely associated with major functions performed by the cell: ion transport and growth.

To study water relations at the level of the single cell, algal model systems are often used because of their large size, accessibility as single cells, and ease of manipulation. Unlike in freshwater algae, which regulate osmotic pressure (Bisson and Bartholomew, 1984), turgor changes in marine or brackish water algae result in chloride (and potassium or sodium) movement. This movement is outward in hypo-osmotic treatments and inward in hyperosmotic treatments, consistent with regulation of turgor by the cell (Bisson and Gutknecht, 1977, 1980; Wendler et al., 1983; Okazaki and Iwasaki, 1992). In general, modification of turgor by external osmotica results in an influx or efflux of ions, changing the osmotic potential of the cell to cause a return to the original turgor. The actual mechanism mediating the response to changes in turgor may involve changes in cytosolic calcium (Okazaki and Iwasaki, 1991; Bisson et al., 1995), possibly triggered by changes in cytoplasmic hydration (Tazawa et al., 1995).

In higher plants, it is known that hyperosmotic treatment causes hyperpolarization of the membrane potential (Kinraide and Wyse, 1986; Li and Delrot, 1987) and extracellular acidification (Reinhold et al., 1984; Curti et al., 1993), which has been attributed to modulation of the proton-pumping activity, resulting in short-term osmoregulation to maintain a constant turgor. Turgor is the "driving force" in cellular expansion. It is clear that the relationship between turgor and growth is complex, involving an interplay between turgor and cell-wall extensibility (Money and Harold, 1992; Cosgrove, 1993). Zhu and Boyer (1992) examined the effect of turgor on growth in *Chara corallina*: Clamping of turgor resulted in transient changes in elongation rate. Turgor modification using external osmotica inhibited growth—this was not observed when turgor was clamped using a pressure probe—raising concerns about the use of external osmotica to modulate turgor. Direct modification (decreases) of turgor with a pressure probe in the freshwater alga *Chara inflata* activates ionic conductances for potassium and chloride as measured by a voltage clamp (Kourie and Findlay, 1991), indicating that turgor can regulate ion transport.

In this paper, we examine the effect of turgor, directly modulated with a pressure probe or indirectly by extracellular osmotica, on the electrical parameters of actively growing higher plant cells. Actively growing root hairs of *Arabidopsis thaliana* were used for the measurements (Lew, 1991) because growth implies that ion transport activity is dynamically maintaining turgor to "drive" cellular expansion (assuming that turgor would otherwise become a limiting condition as the cell expands). A variety of ion transport processes are known to affect Arabidopsis root hair growth. For example, inhibition of the proton pump or potassium channels transiently inhibits growth (Lew, 1991), and calcium currents inward at the hair tip are associated with actively growing root hairs (Schiefelbein et al., 1992). I find that the electrical properties of the cells are

[1] This research was supported by the Natural Sciences and Engineering Research Council of Canada.

* E-mail planters@yorku.ca; fax 1–416–736–5698.

Abbreviation: APW, artificial pond water.

insensitive to direct manipulation of turgor by a pressure probe but are modified by external osmotica. The data are consistent with a "sensor" in these cells, which is not a "turgor-sensor" but instead an "osmo-sensor."

MATERIALS AND METHODS

Seedling Preparation

Seeds of *Arabidopsis thaliana* L. (Columbia wild type) were surface-sterilized with bleach, sown on 0.9 to 1.0% gellan gum (ICN) in APW 5 (0.1 mM KCl, 0.1 mM $CaCl_2$, 0.1 mM $MgCl_2$, 1.0 mM Mes, and 0.2 mM Na_2SO_4, pH-adjusted to 5.0 with NaOH) in tissue culture dishes, and incubated at 25°C under fluorescent lights (350–400 lux). The roots grew along the surface of the gellan gum so that root hairs were accessible for impalement without having to disturb the roots, thus avoiding wounding responses.

After 7 to 14 d, APW 7 (0.1 mM KCl, 0.1 mM $CaCl_2$, 0.1 mM $MgCl_2$, 1.0 mM Mops, and 0.5 mM NaCl, pH-adjusted to 7.0 with NaOH) was added to the culture dishes and impalements were begun after 1 to 3 h. Root hairs were observed every few minutes to ensure that they were elongating (cf. Lew, 1991) and were impaled when they had attained a length of 30 to 100 μm. Growth rates were about 1 μm min^{-1}. Previous experiments demonstrated that growth usually continues after impalement with the microelectrode (Lew, 1991).

Micropipette Fabrication

Double-barreled micropipettes were constructed by placing two borosilicate (KG-33) capillaries with internal filaments (Garner Glass, Claremont, CA) within a nichromium heating filament, heating, and then twisting 360°. The capillaries were then pulled on a vertical pipette puller (model P-30, Sutter, San Rafael, CA). The micropipettes were filled with 3 M KCl. Diffusion of KCl into the cell should not affect the electrical properties of the cell, since even ionophoretic injections of about 200 nanoCoulombs of K^+ or Cl^- are without effect on the membrane potential or current-voltage relations of the cell (data not shown). Pressure-probe micropipettes were pulled using a double-pull protocol to achieve a tip diameter of about 1.5 μm, estimated from light-microscope examination.

Electrophysiology

The micropipette barrels were connected by AgCl electrodes to IE-251 (voltage-clamping electrodes) and IE-201 (electrical coupling experiments) electrometers (input impedance 10^{11} Ω; Warner Instruments, Hamden, CT). After placement in the APW 7, the electrodes were tested for cross-talk by injecting 1 nA of current through one electrode and checking for significant voltage deflections in the other electrode(s); cross-talk was zero to minimal (<5%).

Grounding was via a 2-mm capillary containing 3 M KCl (to match the micropipette KCl concentration) in 2% agar connected to an AgCl electrode. A water immersion objective (see below) was used and caused a secondary shunt to ground. This resulted in minimal additional noise (less than 2.5 mV peak to peak) and did not affect measurements of electrode resistance.

Voltage Clamping

Current-voltage measurements using a voltage clamp (Smith et al., 1980) have been described previously (Lew, 1991). Voltage clamping for current-voltage measurements was computer-driven through a data acquisition board and operational amplifier configured for voltage clamping. With voltage clamps of 500-ms duration, initial activation of clamping current was observed, followed by inactivation (Fig. 1). The initial activation was not a consequence of capacitative coupling between the two barrels of the micropipette, which is complete within less than 5 to 10 ms (data not shown). During the long duration of 500-ms voltage clamps, it was common to see large clamping current surges, possibly due to membrane breakdown. In addition, cytoplasm movement within 10 μm of the micropipette tip, either moving away or toward the tip, depending on current polarity, was often observed. To avoid these multiple artifacts—capacitative cross-talk, membrane breakthrough, and modification of the cytoplasm—a voltage-clamp duration of 50 ms was used.

A bipolar staircase (alternating positive and negative clamps) of voltage clamps followed by a 50-ms voltage clamp at the resting potential minimized any possible hysteresis effects. Data sampling (voltage and current) was performed during the last 10 ms of the voltage clamp, when voltage-inactivated currents had declined approximately 50% (Fig. 1). The plasma membrane H^+ pump

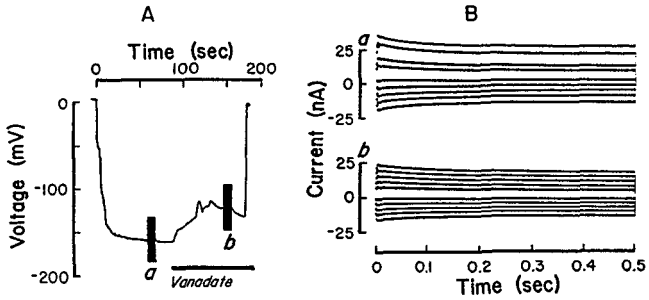

Figure 1. Time dependence of clamping current. A, The double-barreled micropipette (filled with 3 M KCl) was initially pressed against the cell wall (a Donnan potential of −50 mV is commonly observed for the cell wall) and was then impaled into the cell. Long-term voltage clamps, 10 bipolar steps of 500 ms, were performed in the following order: −175, −90, −215, −50, −255, −10, −300, 35, −340, and 75 mV (values are rounded) before (*a*) and after (*b*) 5–10 mM vanadate treatment. B, Clamping currents (*a*, before; *b*, after vanadate treatment) were digitized after filtering at 1 kHz and five data values were averaged to obtain a final sampling rate of 2.87 ms. The clamped voltages from top to bottom for either a or b were 75, 35, −10, −50, −90, −175, −215, −255, −300, and −340 mV. The voltage-dependent inactivation within the first 50 ms of the voltage clamp was commonly observed. This experiment did not have large transients in the clamping current because of membrane breakthrough, but transients and cytoplasmic movement were commonly observed because of long-term current injection.

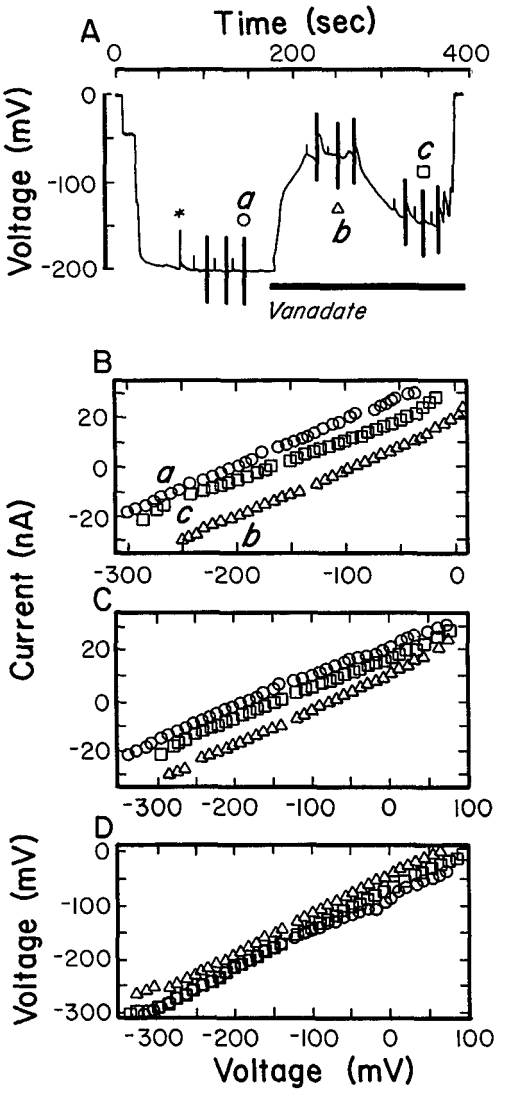

Figure 2. Cable properties of root hairs. Root hairs that were older (i.e. longer) than the ones normally used (to allow a more accurate measurement of the length constant, λ) were impaled with both a double-barreled micropipette (near the tip) and a single-barreled micropipette (near the base). A, The root hair was initially impaled with the double-barreled micropipette as shown. The impalement with the single-barreled micropipette caused a transient depolarization (marked with an asterisk). Current-voltage measurements (40 bipolar steps of 50 ms duration) are marked with vertical bars. Three of these (*a* [○], before vanadate; *b* [△], after 5–10 mM vanadate treatment, depolarized; *c* [□], after vanadate treatment, repolarized) are shown in the three lower panels. The repolarization after vanadate treatment is not always observed. When it does occur, there is a decrease in conductance, indicating a change in plasma membrane transport properties when the H^+ pump is inhibited by vanadate. B, Clamping current from the double-barreled micropipette is compared with the voltage at the single-barreled micropipette. Note that the "clamped" voltage for the single-barreled micropipette (positioned 26 μm closer to the root hair base than the double-barreled micropipette) is lower than that at the double-barreled micropipette (shown in the third panel). C, Clamping current from one barrel of the double-barreled micropipette is compared with the clamped voltage measured in the other barrel. The difference between the current-voltage relations before (*a*) and after (*b*) vanadate treatment shows the typical H^+ pump current, which is normally voltage-independent (i.e. it behaves like a constant-current source) over this voltage range as previously reported (Lew, 1991). This is also observed in B. D, Clamped voltages in the single micropipette are compared with clamped voltages in the double-barreled micropipette. The linearity of the two voltages means that the length constant, λ, is voltage-independent in these young, growing root hairs.

should contribute significantly (based on its expected turnover time of 100 s^{-1}) to the clamping current.

Cable Properties

Estimates of current density are complicated by the cable properties of the root hair (Meharg et al., 1994), electrical coupling between cells (Lew, 1994), and cell geometry. Assuming that the root hair could be considered an ideal cylindrical core conductor of infinite length (Rall, 1977), estimation of current density uses the equation:

$$I_m = I_o/(2\lambda\pi d) \quad (1)$$

where I_m is the current density (A cm^{-2}), I_o is the clamping current (A), λ is the length constant (cm), d is the cell diameter (cm), and the factor 2 accounts for current movement both toward the tip and toward the base of the root hair.

To assess the voltage dependence of the length constant, the cable properties were examined in growing root hairs by impaling them with a double-barreled micropipette toward the end of the root hair and with a single micropipette closer to the epidermal cell part of the root hair. Two sets of experiments were performed: (a) root hair length: 75 ± 12 μm; root hair tip to double-barreled micropipette distance: 26 ± 11 μm; double-barreled micropipette to single-barreled micropipette distance: 22 ± 3 μm (n = 8); and (b) root hair length: 120 ± 11 μm; root hair tip to double-barreled micropipette distance: 50 ± 10 μm; double-barreled micropipette to single-barreled micropipette distance: 42 ± 9 μm (n = 12). The epidermal part of the root hair cell adds about 100 μm to the overall length of the cell. Voltage deflections in both the single-barreled micropipette and the double-barreled micropipette during voltage clamping (Fig. 2) were used to determine the length constant.

The voltage deflections in the double-barreled and single-barreled micropipettes were linearly related (Fig. 2), indicating that the length constant, λ, is voltage-independent in young, growing root hairs. Before inhibition of the major transport activity (the proton pump) by vanadate treatment, the length constant, λ, was 85 μm (n = 19); after vanadate treatment, it was 82 μm (n = 20), an insignificant difference. This value of λ is similar to that reported for older root hairs (on average 558 μm long), about 103 μm (Meharg et al., 1994), except that in older hairs the length constant is apparently voltage-dependent.

As noted above, both cell geometry and electrical coupling may make the assumption of a cylindrical core conductor untenable and may also complicate estimates of current density: (a) The root hair emerges from the epidermal part of the cell, which has a much larger diameter

(about 40 μm compared with 10 μm) that directly affects estimation of the length constant (Equation 1); (b) the impedance of the vacuolar membrane/compartment may create a nonhomogeneous conductive pathway for injected current inside the cell; and (c) the electrical coupling ratio in young (75–120 μm in length), growing root hairs, although voltage-independent (Lew, 1994), is high: about 32 ± 21% (n = 39) (Lew, 1994). Electrical coupling would result in significant current leakage into adjacent cells. Older root hairs (average length of 558 μm) are reported to have much lower coupling ratios (about 5%) (Meharg et al., 1994). (I found the coupling ratio to be 4 ± 2% (n = 8) in older root hairs of 195 to 930 μm length.) Since older root hairs are highly vacuolated, the lower coupling ratios could be due to impalement into the vacuole (Vorob'ev et al., 1982; but see Blatt et al., 1990). In any event, to account for the complications of cell geometry and coupling in estimates of current density, the root hairs would have to be modeled as a highly complex dendritic branching system of coupled cells of varying cylindrical sizes (Rall, 1977; Cao and Abbott, 1993). Clearly, no simple quantitative correction is possible for estimating current density. Qualitative interpretation of the input conductances must take into account current leakage through coupled cells.

Electrical Coupling

Coupling between cells may be regulated by changes in the turgor of one cell. If cell-to-cell coupling were affected, the changes in current leakage could change the magnitude of clamping currents and complicate interpretation of current-voltage relations. Therefore, electrical coupling (Lew, 1994) was also measured. A root hair was impaled with a double-barreled micropipette and an adjacent root hair was impaled with a single-barreled micropipette. A bipolar, 2-nA current pulse train (+2 nA for 1 s, −2 nA for 1 s, and then 0 nA for 1 s) was passed through one of the microelectrodes of the double-barreled assembly, and voltage deflections in the other barrel and in the other micropipette were measured. Coupling percentage was calculated as the voltage deflection in the adjacent cell divided by voltage deflection in the first cell, multiplied by 100.

Microscopy

A microscope (Nikon) was used with a ×40 water immersion objective (NA 0.75) under bright-field conditions. After impalement the image was often recorded on a charge-coupled device video camera (model KP-M1, Hitachi Denshi, Tokyo, Japan) and stored on a video cassette recorder. The images were played back and analyzed using an image processor (model DVS-3000, Hamamatsu, Bridgewater, NJ). Enhancement, when used, involved video frame addition and contrast enhancement; the enhanced images were printed on a video printer (Mitsubishi Electronics America, Somerset, NJ).

Pressure-Probe Measurements

Pressure measurements (Cosgrove et al., 1984; Money, 1990; Zimmerman et al., 1992; Franks et al., 1995) were performed using a subminiature pressure transducer (model XT-140-300G, Kulite Semiconductor Products, Leonia, NJ) housed adjacent to the pressure-probe micropipette in a small brass holder connected to a micrometer-driven piston by thick-walled Teflon tubing (0.159 cm o.d. × 0.0254 cm i.d., Chromatographic Specialties, Brockville, Ontario, Canada). The piston, tubing, holder, and micropipette were filled with silicone oil (polydimethylsiloxane, 2 centistokes, Dow Corning, Midland, MN). The Teflon tubing was required to isolate the pressure probe from vibration during manipulations of the pressure. A drawback of the flexible Teflon tube connection was changes in the tubing size due to pressure application, resulting in slow pressure relaxation.

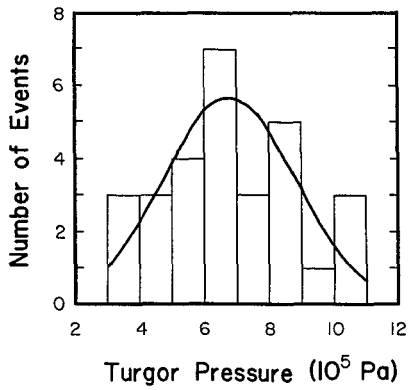

Figure 3. Initial turgor measurements of root hairs. The turgor measurements ranged from 3.0 to 10.6 × 10^5 Pa with a mean ± SD of 6.8 ± 2.0 × 10^5 Pa (n = 29). The curve is a best fit to a Gaussian distribution. Normally, single measurements were performed on a seedling in the early afternoon, so the differences are primarily due to plant-to-plant variability.

After introduction of the pressure probe into the APW 7 solution bathing the root hairs, capillary action filled the tip of the micropipette; this was offset by application of pressure to bring the oil/APW 7 interface to the tip of the micropipette. Pressure was monitored on a digital oscilloscope as voltage output from the transducer using standard electronics. Pressure was calculated based on a calibration performed with pressurized air.

Upon impalement, free movement of the oil/aqueous interface during pressure modulation was an absolute necessity to ensure that plugging of the tip was not affecting the equilibration of pressure between the probe and the cell (Franks et al., 1995). After a pressure pulse was applied, oil movement could continue for a short period (several seconds), indicating some restriction to oil flow at the tip. For example, in measurements of the initial turgor pressure, application of pressure to bring the oil/aqueous interface back to the tip after impalement initially resulted in rapid movement of the interface that slowed and then stopped as it reached the tip, suggesting that equilibration was occurring as the interface reached the tip. Expansion of the Teflon tube would then result in a reversal of the oil movement back into the pressure probe. Longer-term equilibration was not attempted because of time constraints imposed by multiple impalements and the constant

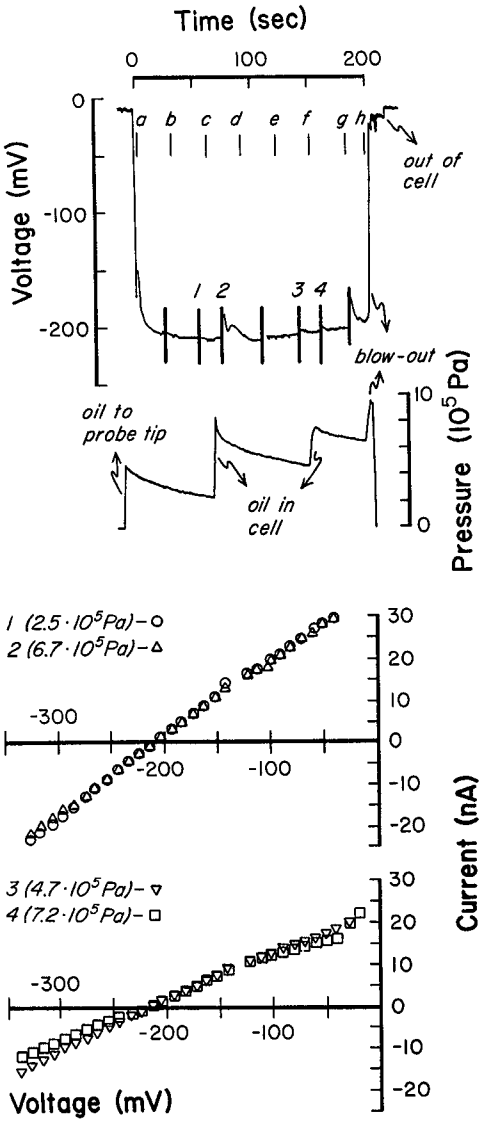

Figure 4. Pressure regulation of root hair electrical properties: Current-voltage measurements. Electrical and pressure-probe measurements (top) were performed by first impaling the root hair with the pressure probe in the highly vacuolate epidermal cell part of the root hair. The oil interface in the probe moved back from the tip upon impalement; it was returned to the tip by applying pressure as shown to obtain a measure of the initial turgor pressure (this was sometimes done after electrical measurements had been made to assess pressure regulation from a "0" turgor pressure). Then, a double-barreled micropipette was impaled into the cytoplasm-rich hair part of the root hair. A stable membrane potential was typically attained quite rapidly, as shown. Video "shots" of this experiment (taken at the points marked *a*, *b*, *c*, etc., and shown in Fig. 5) indicate the relative positioning of the pressure probe and micropipette. Cytoplasmic streaming could be observed after the impalements. Current-voltage measurements (bottom, shown as vertical bars on the electrical trace in the top panel) were performed before and after pressure jumps—confirmed by observing oil movement in the pressure probe and/or oil movement into the cell (Fig. 5, d through h). Relaxation of pressure after the jump was concomitant with a decrease in the amount of oil in the cell—due to very slight stretching of the Teflon tubing connecting the micrometer piston to the probe housing. Pressure jumps from 2.5 to 6.7 × 10^5 Pa (*1* and *2*) and from 4.7 to 7.2 × 10^5 Pa (*3* and *4*) resulted in no consistent change in the conductance (slope) of the current-voltage relations. Blow-out refers to a break in the tip of the root hair that causes violent expulsion of the cell's cytoplasmic contents.

threat of tip-plugging of both the pressure probe and other micropipettes (callose formation at impalement sites is often observed after about 5 min).

RESULTS

Effect of Pressure Modulation by Oil Injection

After ascertaining that the root hair was growing, we inserted the pressure probe into the epidermal part of the root hair. Impalement caused the oil interface in the pressure probe to move back from the tip. The pressure required to bring the interface to the tip was used as a measure of the initial cell turgor (Fig. 3). The turgor pressure, 6.8 ± 2.0 × 10^5 Pa (n = 29), was similar to values reported for *Aster* roots (Zimmerman et al., 1992). The root hair was then impaled with a double-barreled micropipette in the cytoplasm-rich region 10 to 40 μm from the root hair tip (Figs. 4 and 5).

Current-voltage measurements were performed at various points (Fig. 4) while pressure was modulated. Changes in pressure were confirmed by observing whether the oil interface moved and/or whether oil was injected into the cell. If no movement was observed, it was assumed that the pressure-probe tip was blocked and the experiment was then aborted. Figure 5 shows the cell during the experiment at the times marked in Figure 4. Between c and d and again in f through h (Fig. 5), application of pressure resulted in oil injection into the cell, a clear indication of a pressure increase in the cell (Franks et al., 1995). A well-defined interface between the oil and the cellular contents was always observed, indicating that the oil was not dispersing and not affecting cellular contents by mixing. The oil entered the vacuole (location of the pressure-probe tip in the vacuole was confirmed by preliminary experiments in which dextran-conjugated Texas red dye was injected after impalement) and normally resulted in compression of the cytoplasm into the tip of the root hair (Fig. 5, d–h). After oil injection, cytoplasmic streaming could no longer be observed. With sufficient pressure, "blow-out" of the cell occurred. The actual pressure required for blow-out could not be determined since it typically occurred during oil movement into the cell. The site of blow-out was at the tip of the root hair (Fig. 6) and not at the double-barreled micropipette or at the pressure-probe impalement sites. In experiments in which an epidermal cell on an adjacent longitudinal cell file was impaled with the pressure probe, blow-outs occurred at the acropetal end of the cell and not at the pressure-probe impalement site (data not shown).

During the strong modulation of cell turgor pressure and cytological rearrangement, there was no change in either the membrane potential or current-voltage relations (Fig. 4) until blow-out occurred.

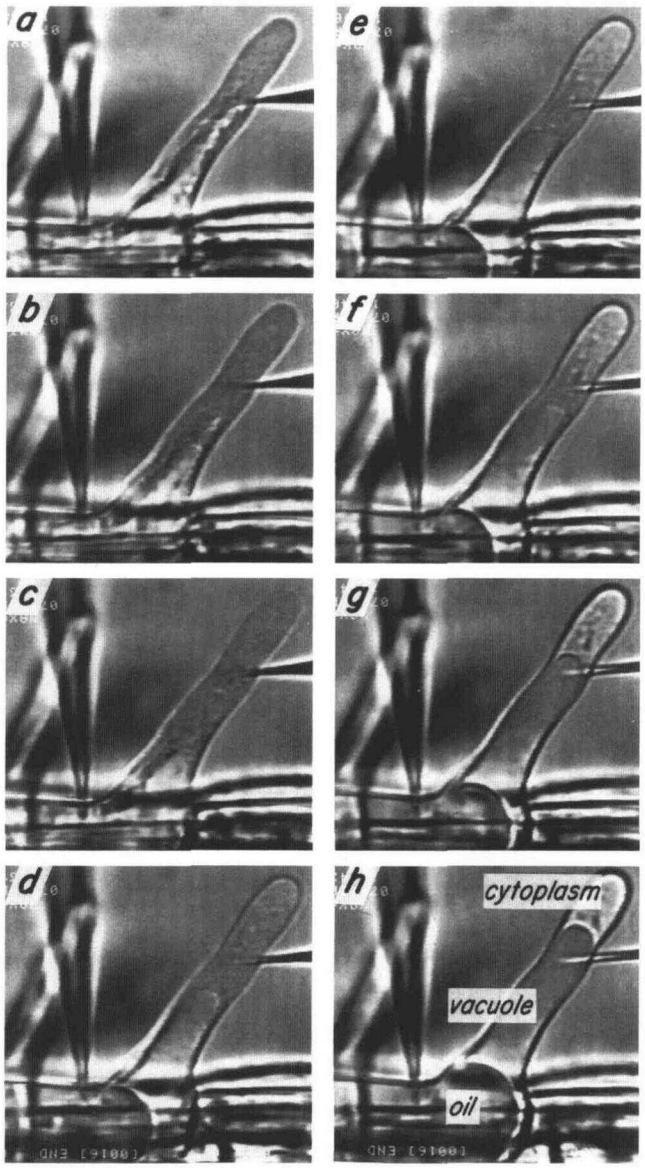

Figure 5. Pressure regulation of root hair electrical properties: Video record. The video shots were 16-frame additions taken at the times marked in Figure 4 (*a, b, c,* etc.). The vacuole extends from the epidermal component of the root hair into the hair component and is clearly distinct from the cytoplasm, being enriched in the hair component, especially at the tip. Under normal circumstances, the shape of the vacuole is pleiomorphic, changing over time as can be seen in a through c. With the introduction of oil (d, corresponding to the first pressure jump in Fig. 4, and f–h, corresponding to the second), the vacuole is "forced" into the cytoplasm-rich hair component of the root hair, causing compression of the cytoplasm. Cytoplasmic streaming, often observable after impalements, ceased after oil injection into the cell. For scale, root hair diameter is about 8 μm.

A compilation of conductance values obtained from current-voltage measurements versus changes in pressure indicated no regulation of conductance by pressure (Fig. 7).

Input-resistance measurements were also carried out to confirm that direct modulation of pressure did not affect ion transport at a faster time resolution (seconds compared with minutes for voltage-clamp experiments). In addition, modification of cell-to-cell coupling by direct modulation of pressure could obscure changes in the conductance of the impaled cell; therefore, the effect of pressure on cell-to-cell coupling was measured using impalements into adjacent cells. An example of an experiment is shown in Figure 8. After impalement of the first, younger root hair with the pressure probe, the same cell was impaled with a double-barreled micropipette. Then the second, older root hair on the same longitudinal cell file, which was connected to the first root hair by an end wall, was impaled with a single-barreled micropipette. This resulted in a

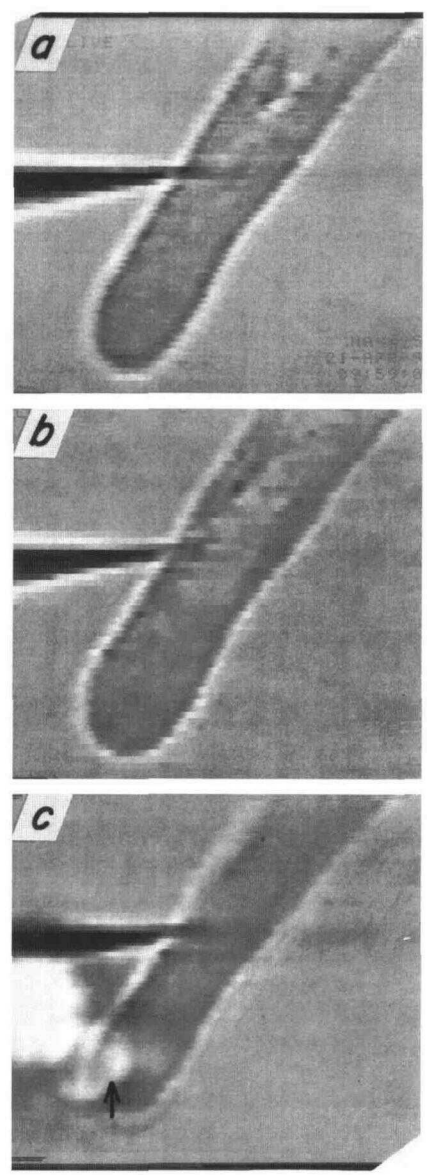

Figure 6. Blow-out of the root hair induced by oil injection. The video "shots" are single frames shown soon after impalement (a), one frame prior to blow-out (b), and at blow-out (c). The lesion where cytoplasm and oil release occurred is marked with an arrow in c. Note the significant bulging of the tip in b, which is not observed in a (prior to oil injection) or c (after release of pressure). For scale, root hair diameter is about 8 μm.

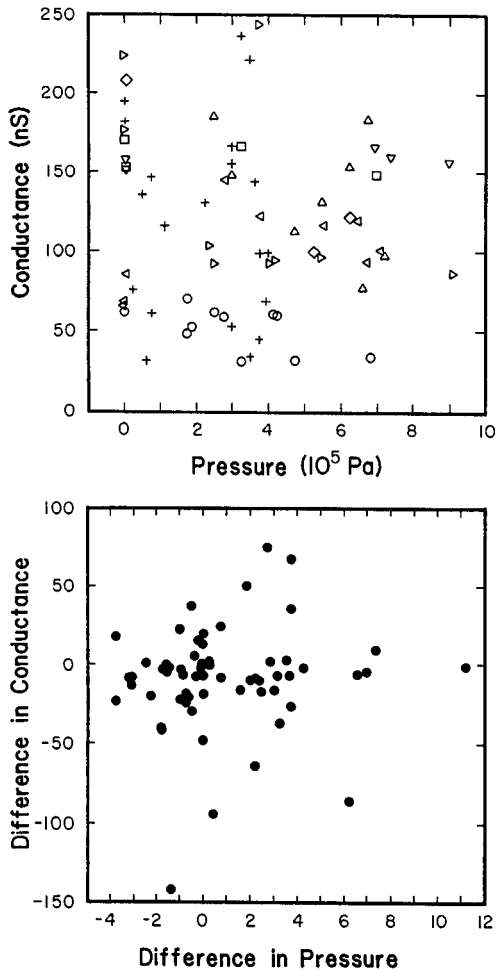

Figure 7. Pressure regulation of root hair electrical properties: Conductance. Conductance was estimated from the slopes of a linear fit of current-voltage relations (which were typically ohmic). Overall, conductance values were 118 ± 55 nS (n = 71). The conductance is compared with root hair turgor pressure modulated by the pressure probe in the top panel (each symbol represents a single experiment). The bottom panel shows the change in conductance (as a difference) versus the change in turgor pressure, compiled from all experiments. Pressure modulation appears to have no effect on conductance: there is no linear trend and changes in conductance cluster around zero. Correlations (r) for individual experiments ranged from −0.46 to 0.44, with a mean value of −0.03.

small transient depolarization of the younger root hair. After preliminary current-voltage measurements, a current pulse train initiated through one barrel of the double-barreled micropipette resulted in voltage deflections in both the younger cell and the older cell. The magnitude of the voltage deflection in the younger cell yields a measurement of the input resistance for that cell. The ratio of voltage deflections in the younger root hair to the deflections in the older root hair, expressed as a percentage, yields a measurement of coupling between the cells.

Application of pressure, confirmed by movement of the oil interface, resulted in no change in either input resistance or coupling (Figs. 8 and 9). Upon blow-out, the younger root hair depolarized almost completely, input resistance increased, and cell-to-cell coupling decreased to 0%. The older root hair transiently depolarized. Similar behavior (transient depolarization after blow-out of an adjacent cell) was also observed when the pressure probe was inserted into an epidermal cell on the longitudinal cell file adjacent to the root hair being measured electrically. Repolarization was concomitant with a decrease in conduc-

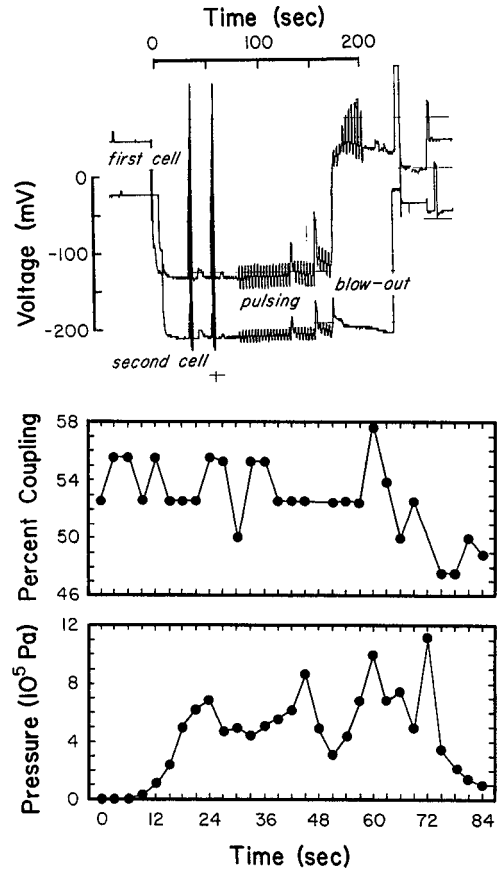

Figure 8. Pressure regulation of root hair electrical properties: Cell-to-cell coupling and input-resistance measurements. Two adjacent root hairs on a longitudinal cell file were impaled: the first, younger cell with a pressure probe and double-barreled micropipette and the second, older cell with a single-barreled micropipette. The membrane potential traces are a direct copy of the experimental record: vertical bars at about 40 and 55 s are current-voltage measurements: voltage deflections in the second cell are a consequence of current leakage through plasmodesmata connecting the two cells. Direct current injection (±2 nA) through one barrel of the double-barreled micropipette in the younger cell results in voltage deflections in both cells. The voltage deflection in the younger cell is a measure of input resistance, and the ratio of the voltage deflections in the older and younger cell yields a measurement of cell-to-cell coupling (percentage of coupling shown in the bottom panel). The 0-s time on the bottom panel refers to the commencement of current pulsing. Soon after pulsing was begun, pressure was modulated by first moving the oil interface to the tip of the pressure probe and then into the cell. When blow-out occurred (after 84 s on the bottom panel) the first cell completely depolarized, the second cell depolarized transiently, and cell-to-cell coupling became zero.

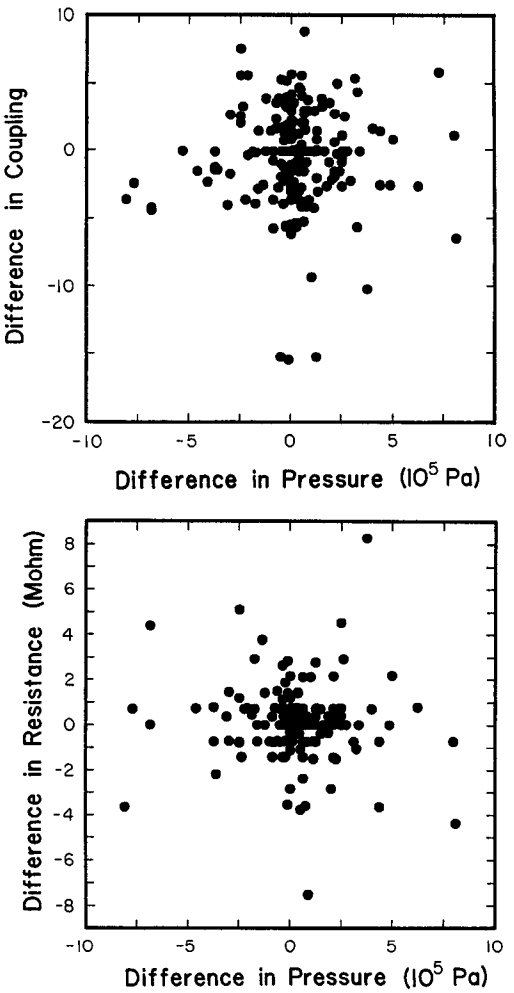

Figure 9. Pressure regulation of root hair electrical properties: Coupling and input resistance. Analogous to the analysis shown in Figure 7, changes in either coupling (top) or input resistance (bottom) compared with changes in turgor pressure are compiled from all experiments. Pressure modulation affects neither parameter: differences in either coupling or input resistance cluster around zero, with no indication of a linear trend.

tance, consistent with a loss of cell-to-cell coupling (data not shown).

Analogous to the lack of any effect of direct modulation of turgor pressure on conductance (Fig. 7), the relationship between changes in pressure and either input resistance or cell-to-cell coupling (Fig. 9) indicates that direct modulation of pressure affected neither property of the root hair.

Effect of Pressure Modulation by Extracellular Osmoticum

Although there are reports of osmoticum-induced changes in the membrane potential of higher plant cells (Kinraide and Wyse, 1986; Li and Delrot, 1987), it is possible that the electrical properties of root hairs—membrane potential, conductance, input resistance, and cell-to-cell coupling—were unaffected by changes in turgor pressure because the root hairs simply lack any turgor regulation. Therefore, the effect of indirect modulation of turgor by extracellular osmotica was examined.

The osmoticum was 100 mM mannitol plus 100 mM sorbitol (200 mM mannitol/sorbitol) in APW 7 solution. The concentration of osmoticum corresponds to a pressure change of 4.8×10^5 Pa (from the Van't Hoff relation), which is within the range of pressure changes performed directly with the pressure probe.

Two protocols were performed: (a) hypo-osmotic effects were examined by pretreatment in APW 7 plus 200 mM mannitol/sorbitol—after impalement, treatment with APW 7 was given; and (b) hyperosmotic effects were examined by pretreatment with APW 7—after impalement, treatment with APW 7 plus 200 mM mannitol/sorbitol was given. In either case, only growing root hairs were used. In the case of pretreatment with APW 7 plus 200 mM mannitol/sorbitol, there was an unusual delay before root hairs began growing, and they exhibited some atypical morphological variations: greater than normal diameter and variable bulging along the root hair. Initial turgor measured in one cell was 3.6×10^5 Pa. Although tip growth can be maintained at this external osmolarity, the root hairs exhibited a morphological response to the presence of osmoticum.

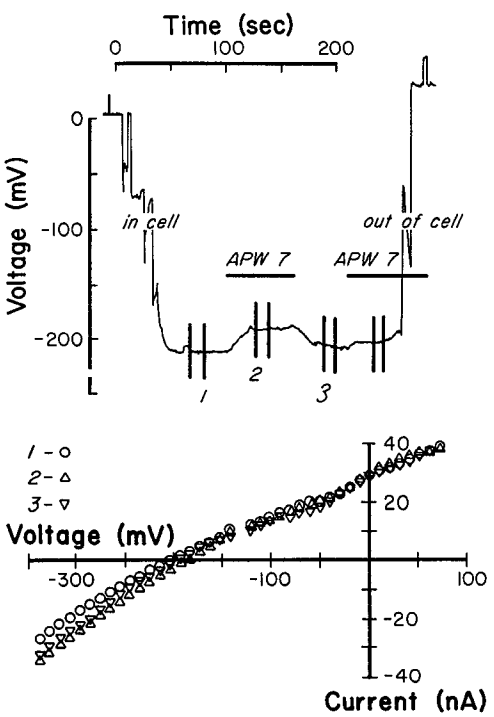

Figure 10. Osmotic regulation of root hair electrical properties: Hypo-osmotic treatment. The root hairs were pretreated with APW 7 plus 200 mM mannitol/sorbitol and were then treated with APW 7 alone during the times marked by horizontal bars in the top panel. This hypo-osmotic treatment caused depolarization of the membrane potential and increased conductance as seen in the current-voltage measurements in the bottom panel taken before (*1*), during (*2*), and after (*3*) the first treatment with APW 7 alone, at the times indicated in the top panel.

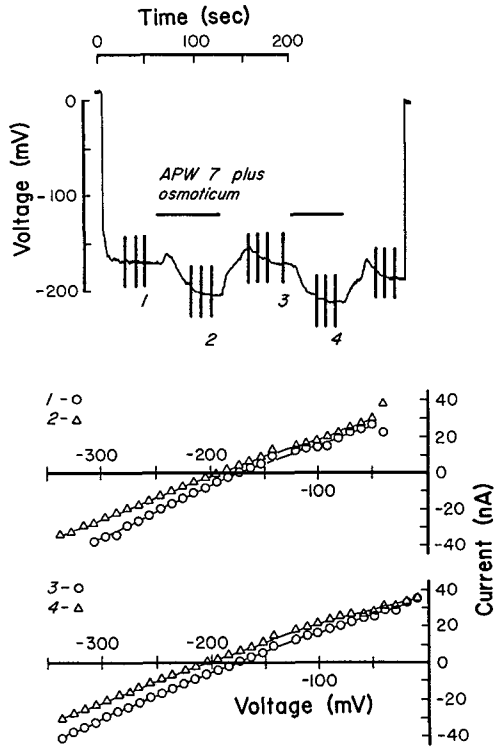

Figure 11. Osmotic regulation of root hair electrical properties: Hyperosmotic treatment. The root hairs were pretreated with APW 7 and were then treated with APW 7 plus 200 mM mannitol/sorbitol during the times marked by horizontal bars in the top panel. This hyperosmotic treatment caused hyperpolarization of the membrane potential and decreased conductance, as seen in the current-voltage measurements in the bottom panel taken before and during the first (*1* and *2*) and second (*3* and *4*) treatments with APW 7 plus 200 mM mannitol/sorbitol at the times indicated in the top panel.

Hypo-osmotic treatment with APW 7 caused a depolarization of 38 ± 13 mV (n = 17) from the initial potential of −192 ± 29 mV. The depolarization was reversed by a return to APW 7 plus 200 mM mannitol/sorbitol (n = 8; Fig. 10). An increase in conductance (Figs. 10 and 12) was commonly observed. The initial conductance was 153 ± 22 nS (n = 15), and hypo-osmotic treatment caused an increase in conductance of 24 to 177 ± 36 nS, a statistically significant difference (Tukey test, P = 0.002). To ensure that the increase in conductance was not due to an increase in cell-to-cell coupling, coupling was measured as in Figure 8 and was not significantly different before (52 ± 13%) or after (50 ± 12%) hypo-osmotic treatments (n = 4). With 150-ms voltage clamps analogous to those shown in Figure 1, no consistent change in time dependence of the clamping currents was observed (data not shown).

Hyperosmotic treatment with APW 7 plus 200 mM mannitol/sorbitol caused a hyperpolarization of 25 ± 8 mV (n = 22) from an initial potential of −189 ± 15 mV. The hyperpolarization was reversed by a return to APW 7 (six of seven experiments). In this case a decline in conductance was commonly observed (Figs. 11 and 12). The initial conductance of 190 ± 40 nS decreased 22 nS to 167 ± 41 nS (n = 20). The decrease in conductance was significantly different (Tukey test, P = 0.006). Cell-to-cell coupling was not significantly affected by hyperosmotic treatment (before, 62 ± 8%; after, 59 ± 8%; n = 5) and therefore was not the cause of the decrease in conductance. No consistent change in time-dependent clamping currents was observed (data not shown).

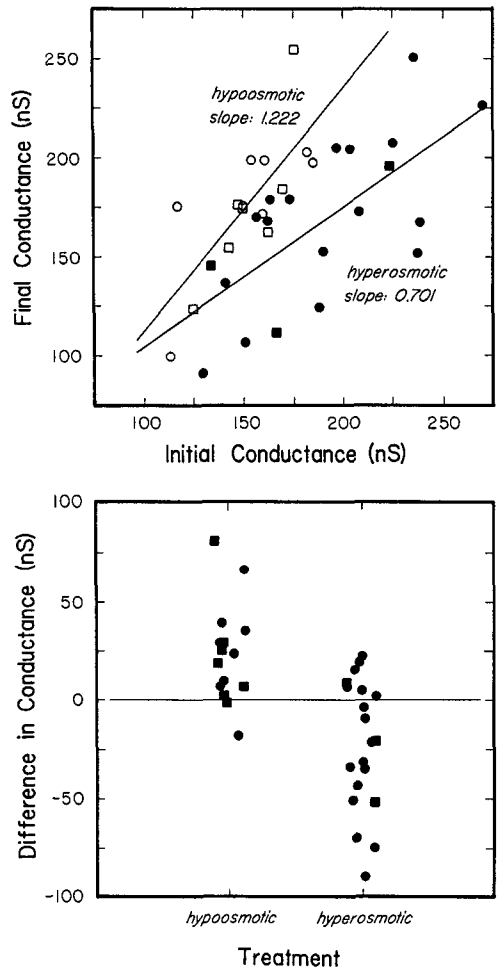

Figure 12. Osmotic regulation of root hair electrical properties: Conductance. Conductances were estimated from the slopes of linear fits of the current-voltage relations for 50-ms voltage-clamp experiments (circles) and time-dependent clamping current experiments (using the clamping current values at 50 ms; squares). The final conductances (measured after osmotic treatment) are plotted against the initial conductances (measured before osmotic treatment) in the top panel (hypo-osmotic treatment, empty symbols; hyperosmotic treatment, filled symbols). Linear regressions for each treatment are also shown as marked. Hypo-osmotic treatment caused a 22% increase in conductance, and hyperosmotic treatment caused a 30% decrease. For each experiment the difference in conductance before and after osmotic treatment is shown in the bottom panel (data are "jittered" to improve visibility). Hypo-osmotic treatment resulted in a 24 ± 24 nS increase in conductance (n = 15); hyperosmotic treatment resulted in a 22 ± 32 nS decrease in conductance (n = 20). Both effects were highly significant using either a Tukey test (P < 0.007 for either treatment) or the nonparametric Wilcoxon test (P < 0.016 for either treatment).

The results indicate that direct modulation of turgor with a pressure probe affects neither the electrical properties of the root hairs—potential, conductance, and input resistance—nor cell-to-cell coupling. Indirect modulation of turgor by changes in extracellular osmolarity causes depolarization and increased conductance for hypo-osmotic treatment, and hyperpolarization and decreased conductance for hyperosmotic treatment, but cell-to-cell coupling is unaffected. Although direct and indirect treatments both result in changes in turgor pressure, the cell appears to be able to sense only indirect modulation of turgor, indicating that the sensing mechanism is an osmo-sensor and not a turgor-sensor.

DISCUSSION

The process of osmoregulation can be conceptually divided into three steps: sensing, transduction, and response. Responses may be either short term, such as immediate changes in ion fluxes, or long term, such as de novo synthesis of osmotically active metabolites (Kauss, 1983). Transduction may involve kinase activity (Brewster et al., 1993) or calcium transients (Tazawa et al., 1995).

There are also some indications pointing to the mechanism of turgor sensing. In bacteria, stretch-activated channels have been implicated: gadolinium inhibits both stretch-activated channel activity and loss of ions and metabolites in response to hypo-osmotic treatment (Berrier et al., 1992), whereas a two-component sensor-effector system activating K^+ uptake has been implicated in hyperosmotic treatment (Walderhaug et al., 1992). Stretch-activated channels do occur in higher plants (Cosgrove and Hedrich, 1991), but in other organisms such as *Neurospora crassa* inhibition of stretch-activated channels by gadolinium does not increase the extent of hypo-osmotic-induced lysing of hyphae (Levina et al., 1995); therefore, they may not always play a role in sensing hypo-osmotic stress. In general, it is likely that there is a wide variation in the mechanisms involved in all three aspects of osmoregulation.

Originally, the experiments performed here were intended to obtain evidence of ion transport regulation by turgor changes in higher plant cells. With root hairs known to be actively growing, ion transport is expected to play a role in maintaining turgor during cellular expansion (Lew, 1991). The turgor in turn would "drive" cellular expansion in concert with modulation of cell-wall extensibility (Money and Harold, 1992; Cosgrove, 1993). It is already clear that a variety of ion transport processes occur during the process of cellular expansion: the plasma membrane proton pump and electrophoretic K^+ uptake are both active; when either is inhibited, growth is inhibited transiently (Lew, 1991). Furthermore, inward Ca^{2+} currents at the root hair tip are observed only in growing hairs; indeed, external Ca^{2+} is required for growth (Schiefelbein et al., 1992). Based on the demonstration of a tip-high gradient of stretch-activated Ca^{2+}-permeable channels implicated in tip growth and maintenance of a tip-high gradient of cytosolic Ca^{2+} in the oomycete *Saprolegnia ferax* (Garrill et al., 1993), it is tempting to believe that the inward Ca^{2+} current results from the activity of stretch-activated channels located at the growing tip of the root hair. In addition, a role of stretch-activated channels in turgor regulation has been suggested for guard cells (Cosgrove and Hedrich, 1991). With growing root hairs, it was expected that an interplay between turgor and ion transport would be observed.

Direct modulation of turgor pressure in root hairs during measurements of electrical activity is technically challenging. The pressure-probe tip must be large to allow free movement of solution through the tip; avoiding damage to the cell during impalement is essential. In addition, multiple impalement sites are required to obtain measurements of the electrical properties and cell-to-cell coupling. However, the impalement sites encompass a relatively small percentage of the overall surface area of the cell. The electrical properties of the cells (membrane potentials in the range of −170 to −190 mV and conductances in the range of 100 to 200 nS) are similar to previous measurements (Lew, 1991, 1994). Cell-to-cell coupling (in the range of 50–60%) tended to be higher than previously reported values (about 30%; Lew, 1994). With multiple impalements the membrane potential returns to its original level; additional impalement sites do not introduce a significant low resistance shunt between the intracellular and extracellular environments. Furthermore, blow-out did not occur at impalement sites, indirectly demonstrating their structural integrity.

Pressure modulation by oil injection caused very significant changes in internal turgor. The result was (a) severe rearrangement of cytoplasmic structure, particularly movement of cytoplasm into the root hair tip; (b) bulging of the tip, which would be expected to cause activation of mechanosensitive channels; and (c) cessation of cytoplasmic streaming. Even with these changes there was no indication that ion transport was affected: no changes in net charge movement that would affect the membrane potential, no increased total ion movement that would affect membrane conductance, and no change in cell-to-cell coupling. Cellular regulation of ion transport and plasmodesmatal connections clearly appear to be insensitive to direct turgor modulation.

Responsiveness to turgor modulation could be demonstrated when the modulation was performed indirectly by changing the extracellular osmolarity. In this case, the results confirm previous reports (Kinraide and Wyse, 1986; Li and Delrot, 1987). In hypo-osmotic treatments, the depolarization and increased conductance are consistent with increased ion efflux from the cell, with Cl^{-1} a likely candidate. In hyperosmotic treatments, both hyperpolarization and decreased conductance were observed. It is common to implicate activation of the proton pump when hyperpolarizations are seen; however, if this were the case, activation of the pump would be expected to have either no effect or cause an increase in conductance due to increased ion efflux across the plasma membrane. Instead, the conductance declined, consistent with a decrease in steady-state ion uptake into the cell, with K^+ a likely candidate (Blatt,

1988; Lew, 1991). That these changes are only observed when turgor is modulated by changes in extracellular osmotica and not when the pressure probe is used indicates that the immediate sensor is an osmo-sensor, possibly located external to the plasma membrane.

SUMMARY

Multiple impalements to assess a full range of the electrical properties of actively growing root hairs have been used to demonstrate that an osmo-sensor rather than a turgor-sensor mediates immediate responses to changes in the water relations of the cell. These changes include hypo-osmotic-induced depolarization and increased conductance, consistent with increased ion efflux from the cell, and hyperosmotic-induced hyperpolarization and decreased conductance, consistent with decreased ion transport across the plasma membrane. One implication of this result is that experimental analysis of the relationship between turgor and growth should rely on direct modulation of turgor with a pressure probe to avoid activating the osmo-sensor. The presence of an osmo-sensor implies a physical mechanism of transduction quite different from that expected for a turgor-sensor, possibly relying on shifts in the osmolarity of the cell wall/plasma membrane interface.

Received May 17, 1996; accepted July 26, 1996.

LITERATURE CITED

Berrier C, Coulombe A, Szabo I, Zoratti M, Ghazi A (1992) Gadolinium ion inhibits loss of metabolites induced by osmotic shock and large stretch-activated channels in bacteria. Eur J Biochem **206:** 559–565

Bisson MA, Bartholomew D (1984) Osmoregulation or turgor regulation in *Chara*? Plant Physiol **74:** 252–255

Bisson MA, Gutknecht J (1977) Osmotic regulation in the marine alga, *Codium decorticatum*. II. Active chloride efflux exerts negative feedback control on the turgor pressure. J Membr Biol **37:** 85–98

Bisson MA, Gutknecht J (1980) Osmotic regulation in algae. *In* RM Spanswick, WJ Lucas, J Dainty, eds, Plant Membrane Transport: Current Conceptual Issues. Elsevier/North Holland Biomedical Press, Amsterdam, The Netherlands, pp 131–142

Bisson MA, Kiegle E, Black D, Kiyosawa K, Gerber N (1995) The role of calcium in turgor regulation in *Chara longifolia*. Plant Cell Environ **18:** 129–137

Blatt MR (1988) Mechanism of fusicoccin action: a dominant role for secondary transport in a higher-plant cell. Planta **174:** 187–200

Blatt MR, Thiel G, Trentham DR (1990) Reversible inactivation of K^+ channels of *Vicia* stomatal guard cells following the photolysis of caged inositol 1,4,5-trisphosphate. Nature **346:** 766–769

Brewster JL, de Valoir T, Dwyer ND, Winter E, Gustin MC (1993) An osmosensing signal transduction pathway in yeast. Science **259:** 1760–1763

Cao BJ, Abbott LF (1993) A new computational method for cable theory problems. Biophys J **64:** 303–313

Cosgrove D (1986) Biophysical control of plant cell growth. Annu Rev Plant Physiol **37:** 377–405

Cosgrove DJ (1993) Water uptake by growing cells: an assessment of the controlling roles of wall relaxation, solute uptake, and hydraulic conductance. Int J Plant Sci **154:** 10–21

Cosgrove DJ, Hedrich R (1991) Stretch-activated chloride, potassium and calcium channels coexisting in plasma membranes of guard cells of *Vica faba* L. Planta **186:** 143–153

Cosgrove DJ, Van Volkenburgh E, Cleland RE (1984) Stress relaxation of cell walls and the yield threshold of growth. Demonstration and measurement by micro-pressure probe and psychrometer techniques. Planta **162:** 46–54

Curti G, Massardi F, Lado P (1993) Synergistic activation of plasma membrane H^+-ATPase in *Arabidopsis thaliana* cells by turgor decrease and by fusicoccin. Physiol Plant **87:** 592–600

Franks PJ, Cowan IR, Tyerman SD, Cleary AL, Lloyd J, Farquhar JD (1995) Guard cell pressure/aperture characteristics measured with a pressure probe. Plant Cell Environ **18:** 795–800

Garrill A, Jackson SL, Lew RR, Heath IB (1993) Ion channel activity and tip growth: tip-localized stretch-activated channels generate an essential Ca^{2+} gradient in the oomycete *Saprolegnia ferax*. Eur J Cell Biol **60:** 358–365

Kauss H (1983) Volume regulation in *Poterioochromonas*. Involvement of calmodulin in the Ca^{2+}-stimulated activation of isofloridoside-phosphate synthase. Plant Physiol **71:** 169–172

Kinraide TB, Wyse RE (1986) Electrical evidence of turgor inhibition of proton extrusion in sugar beet taproot. Plant Physiol **82:** 1148–1150

Kourie JI, Findlay GP (1991) Ionic currents across the plasmalemma of *Chara inflata* cells. III. Water-relations parameters and their correlation with membrane electrical properties. J Exp Bot **42:** 151–158

Kramer PJ (1983) Water Relations of Plants. Academic Press, New York

Levina NN, Lew RR, Hyde GJ, Heath IB (1995) The roles of Ca^{2+} ions and plasma membrane ion channels in hyphal tip growth of *Neurospora crassa*. J Cell Sci **108:** 3405–3417

Lew RR (1991) Electrogenic transport properties of growing *Arabidopsis* root hairs. The plasma membrane proton pump and potassium channels. Plant Physiol **97:** 1527–1534

Lew RR (1994) Regulation of electrical coupling between *Arabidopsis* root hairs. Planta **193:** 67–73

Li Z-S, Delrot S (1987) Osmotic dependence of the transmembrane potential difference of broadbean mesocarp cells. Plant Physiol **84:** 895–899

Meharg AA, Maurousset L, Blatt MR (1994) Cable corrections of membrane currents recorded from root hairs of *Arabidopsis thaliana* L. J Exp Bot **45:** 1–6

Milthorpe FL, Moorby J (1974) An Introduction to Crop Physiology. Cambridge University Press, Cambridge, UK

Money NP (1990) Measurement of hyphal turgor. Exp Mycol **14:** 416–425

Money NP, Harold FM (1992) Extension growth of the water mold *Achlya*: interplay of turgor and wall strength. Proc Natl Acad Sci USA **89:** 4245–4249

Okazaki Y, Iwasaki N (1991) Injection of a calcium-chelating agent into the cytoplasm retards the progress of turgor regulation upon hypotonic treatment in the alga *Lamprothanium*. Plant Cell Physiol **32:** 185–194

Okazaki Y, Iwasaki N (1992) Net efflux of Cl^- during hypotonic turgor regulation in a brackish water alga *Lamprothanium*. Plant Cell Environ **15:** 61–70

Passioura JB (1988) Water transport in and to roots. Annu Rev Plant Physiol Plant Mol Biol **39:** 245–265

Rall W (1977) Core conductor theory and cable properties of neurons. *In* ER Kandel, ed, Handbook of Physiology, Vol 1. American Physiological Society, Bethesda, MD, pp 39–97

Reinhold L, Seiden A, Volokita M (1984) Is modulation of the rate of proton pumping a key event in osmoregulation? Plant Physiol **75:** 846–849

Schiefelbein JW, Shipley A, Rowse P (1992) Calcium influx at the tip of growing root-hair cells of *Arabidopsis thaliana*. Planta **187:** 455–459

Smith TG Jr, Barker JL, Smith BM, Colburn TR (1980) Voltage clamping with microelectrodes. J Neurosci Methods **3:** 105–128

Tazawa M, Shimada K, Kikuyama M (1995) Cytoplasmic hydration triggers a transient increase in cytoplasmic Ca^{2+} concentration in *Nitella flexilis*. Plant Cell Physiol **36:** 335–340

Vorob'ev LN, Tarkhanov KA, Vakhmistrov DB (1982) Use of electrical coupling factor for quantitative estimation of symplastic communications. Sov Plant Physiol **28:** 495–502

Walderhaug MO, Polarek JW, Voelkner P, Daniel JM, Hesse JE, Altendorf K, Epstein W (1992) KdpD and KdpE, proteins that control expression of the kdpABC operon, are members of the two-component sensor-effector class of regulators. J Bacteriol **174:** 2152–2159

Wendler S, Zimmerman U, Bentrup FW (1983) Relationship between cell turgor pressure, electrical membrane potential, and chloride efflux in *Acetabularia mediterranea.* J Membr Biol **72:** 75–84

Zhu GI, Boyer JS (1992) Enlargement in *Chara* studied with a turgor clamp. Growth rate is not determined by turgor. Plant Physiol **100:** 2071–2080

Zimmerman U, Rygol J, Balling A, Klock G, Metzler A, Haase A (1992) Radial turgor and osmotic pressure profiles in intact and excised roots of *Aster tripolium.* Plant Physiol **99:** 186–196